XXI IMEKO World Congress "Measurement in Research and Industry"
August 30 - September 4, 2015, Prague, Czech Republic

REPEATABILITY OF LASER-DOPPLER VELOCIMETRY EXPERIMENTS FOR INDUSTRIAL PIPE-FLOW ANALYSIS

Denis F. Hinz [1]

[1] Kamstrup A/S, 8660 Skanderborg, Denmark, dfh@kamstrup.com

Abstract - We study the repeatability of laser-Doppler velocimetry experiments for pipe-flow analysis. For single-point velocity measurements, we find repeatability standard deviations of approximately $0.5\,\%$ in the core region whereas measurements close to the wall are de-facto unrepeatable. We discuss how repeatability data may be used to verify uncertainty budgets and how it could be included in revised uncertainty budgets in view of established guidelines such as GUM and ISO 21748.

Keywords: Laser-Doppler velocimetry, turbulent pipe-flow, repeatability, uncertainty, statistical error, GUM, ISO 21748.

1. BACKGROUND AND INTRODUCTION

The application of Laser-Doppler velocimetry (LDV) for pipe-flow analysis has considerable potential to support the development and validation of calibration benches for water, heat, and cooling meters. For example, LDV has prospective for qualitative diagnosis of flow conditions on calibration benches [13], for the investigation of installation effects in pipe-flow [14, 15], and as an in-situ calibration method for heat and water meters in operation [5, 10–12].

The combined uncertainty of single-point LDV measurements as well as an estimated volume flow-rate Q_m has been established through detailed uncertainty budgets that account for various systematic and random uncertainty contributions [3–7]. These uncertainty analyses are commonly based on the *Guide to the Expression of Uncertainty in Measurement* [1] (GUM) approach, also referred to as "bottom-up" approach, that amounts to estimating the combined uncertainty from variances associated with the input parameters of the underlying mathematical model. Complementary to the "bottom-up" approach, experimental uncertainty evaluation amounts to conducting "top-down" uncertainty estimates through repeatability and reproducibility studies (cf., e.g., ISO 21748 [2]). However, such "top-down" repeatability studies of LDV experiments appear to be unavailable and uncertainty budgets of LDV systems [3–7] do not explicitly account for the notion of repeatability relating to the entire measurement process rather than the uncertainty of an individual result. Yet, the overall repeatability as a measure of the consistency of LDV systems to achieve identical results across repeated experiments is key to enable a reliable interpretation of experimental data. This is particularly important for the mentioned metrology applications, where qualitative *and* quantitative information is sought.

As a step towards a thorough experimental uncertainty analysis, we focus on quantifying the repeatability of LDV experiments. To this end, we conduct a series of LDV experiments for pipe-flow analysis in industrial applications. As a field test with realistic conditions, we choose the representative example of measurements for the diagnosis of flow conditions in flow benches used for the calibration and verification of water, heat, and cooling meters. Using this experimental setup, we quantify the overall repeatability of LDV measurements through various consecutive measurements under repeatability conditions [1, 2]. Following the GUM [1], we define repeatability as the "closeness of the agreement between the results of successive measurements of the same measurand carried out under the same conditions of measurement". We quantify repeatability in terms of the dispersion characteristics of the results obtained from LDV experiments under repeatability conditions. In the following, *measurand* is used interchangeably with *quantity*.

We note that experiments under reproducibility conditions are likely to provide additional experimental evidence for a thorough "top-down" uncertainty analysis, but are beyond the scope of this article. However, performing reproducibility experiments in addition to this repeatability study might well be worth the effort and should be subject to future investigations.

2. MATERIAL AND METHODS

We use a commercial shifted Nd:YAG LDV probe from ILA/Optolution. Following best-practice guidelines, the settings and parameters of the LDV system are determined based on the expected characteristic velocity of the experiment. For the present experiments, we use flow seeding with neutrally buoyant silver-coated hollow glass beads, a shift frequency $f_{\mathrm{shift}} = 5.0\,\mathrm{MHz}$, $70.0\,\mathrm{mW}$ laser power with a wavelength of $\lambda = 532.0\,\mathrm{nm}$, and a lense with with $f = 120\,\mathrm{mm}$ focal length and associated fringe distance of $d = 1.433\,\mu\mathrm{m}$, where the fringe distance has been calibrated with the spinning disk method. The signal is first treated with hardware high-pass and low-pass band filters where $f_{\mathrm{Hi}} = 0.1\,\mathrm{MHz}$ and $f_{\mathrm{Lo}} = 20.0\,\mathrm{MHz}$.

Individual bursts are triggered from the input signal based on the selection of a trigger level. We select an input range of $\pm 2.0\,\mathrm{V}$ and a trigger level of $+50.0\,\%$. To drop bursts at spurious frequencies, valid

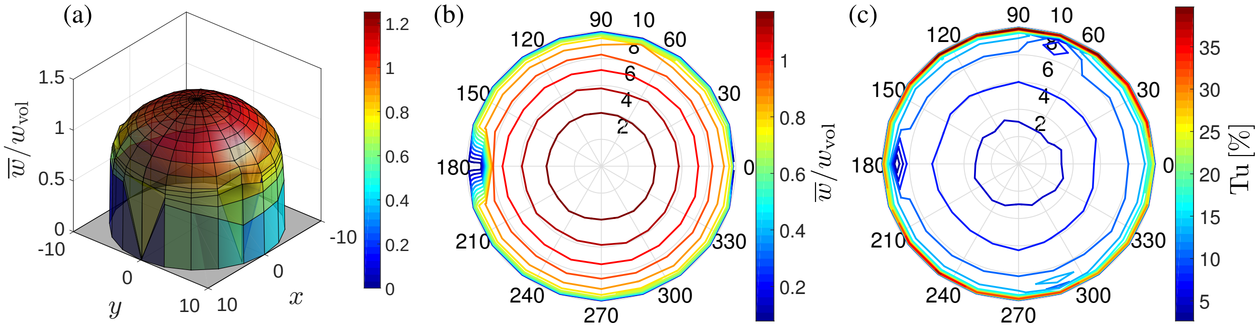

Fig. 1. Representative normalized axial velocity profiles and turbulence intensities of LDV measurements at $\mathrm{Re} = 4 \cdot 10^4$ for $T = 20.0°$ C and $D = 20.0\,\mathrm{mm}$. (a–b) Normalized axial velocity profile $\overline{w}/w_{\mathrm{vol}}$ and (c) turbulence intensity Tu.

bursts are determined through hard frequency cutoffs with $1.0\,\mathrm{MHz} < \mathrm{f_D} < 6.0\,\mathrm{MHz}$, a minimum amplitude ratio of 3.0 between the first and the second peak, and a signal threshold of $1.0 \cdot 10^{-4}$, where the spectral analysis is realized with a sample rate of $25.0\,\mathrm{MHz}$ and 1024 samples (512 pre-trigger and 512 post-trigger).

In the present study, the amount of data acquired at each measurement point is determined by the choice of two experimental constraints: (I) the maximal number of single-point samples $n_{\max}$ and (II) a timeout $t_{\max}$ for each single-point measurement on the measurement grid. For the present measurements we choose

$$n_{\max} = 10^3 \quad \text{and} \quad t_{\max} = 60.0\,\mathrm{s}. \tag{1}$$

All experiments are performed on a calibration flow bench with an expanded uncertainty of $0.30\,\%$ (coverage factor $k = 2.0$) for measurements against weight with test-volumes of $3\,\mathrm{liter}$ to $100\,\mathrm{liter}$. The flow bench is equipped with three magneto-inductive (MID) master meters, each one responsible for a certain flow-rate interval. All experiments are performed with water at $20.0\,°\mathrm{C}$ and brass pipes with diameter $D = 20.0\,\mathrm{mm}$, giving the Reynolds number $\mathrm{Re} = 4.0 \cdot 10^4$, where $\mathrm{Re} = w_{\mathrm{vol}} D/\nu$, $w_{\mathrm{vol}} = Q/A$, and $\nu = 1004.79 \cdot 10^{-9}\,\mathrm{m/s}$. To achieve undisturbed flow conditions, all experiments are performed with an inlet length of $L = 100.0D$.

The volume flow-rate Q, the water temperature T, and the pressure p are stabilized through PID controlled feedback loops. We verify the stability of Q, T, and p by logging data from the master meters and the corresponding temperature and pressure sensors, where $\overline{Q}_M$ is the time-averaged master flow-rate and σ_{Q_M} is the associated standard deviation providing a measure for the stability of the flow-rate. We find $\sigma_{Q_M}/\overline{Q}_M = 0.25\,\%$ and the master meter signal has the characteristics of random white noise, which confirms that there is no preferred timescale and no low frequency disturbances that might bias the long-time accuracy of LDV measurements.

Characteristic results from a representative measurement at $\mathrm{Re} = 4.0 \cdot 10^4$ are shown in Fig. 1. Visual inspection confirms that the flow is fully developed and without major disturbances. With the exception of a few measurement points, the measured flow profiles are smooth and closely approximate the theoretical profiles of Gersten and Herwig [8, 9] for turbulent flow (Fig. 2). The points at which the velocity spuriously drops to zero or values close to zero correspond to points where no signal or only weak signals could be obtained due to optical disturbances and reflections.

3. REPEATABILITY OF LDV EXPERIMENTS

We determine the repeatability of local quantities and global quantities. Local quantities are single-point measurements of the local axial mean velocity $\overline{w}$ and the associated single-point turbulence intensity Tu. To determine $\overline{w}$, we use the estimator

$$\overline{w} = \frac{1}{n} \sum_{i=1}^{n} w_i, \tag{2}$$

with w_i single-point samples of velocities and n the number of samples. The associated single-point turbulence intensity is

$$\mathrm{Tu} = \frac{\sigma_w}{\overline{w}}, \tag{3}$$

where

$$\sigma_w = \left(\frac{1}{n-1} \sum_{i=1}^{n} (w_i - \overline{w})^2 \right)^{1/2} \tag{4}$$

is the standard deviation of samples w_i.

Conversely, global quantities are inferred from the local quantities of the LDV experiments through additional post-processing steps. For example, an integration of the individual point measurements $\overline{w}$ on a measurement grid in polar coordinates yields the volume flow-rate

$$Q_m = \int_0^{2\pi} \int_0^{R} \overline{w} r \, \mathrm{d}r \mathrm{d}\varphi. \tag{5}$$

Our choice of measurement grid contains $N_\theta = 10$ individual (2D) profiles through radial paths. The counterpart of (5) for one measurement path is

$$Q_i = 2\pi \int_0^{R} \overline{w} r \, \mathrm{d}r. \tag{6}$$

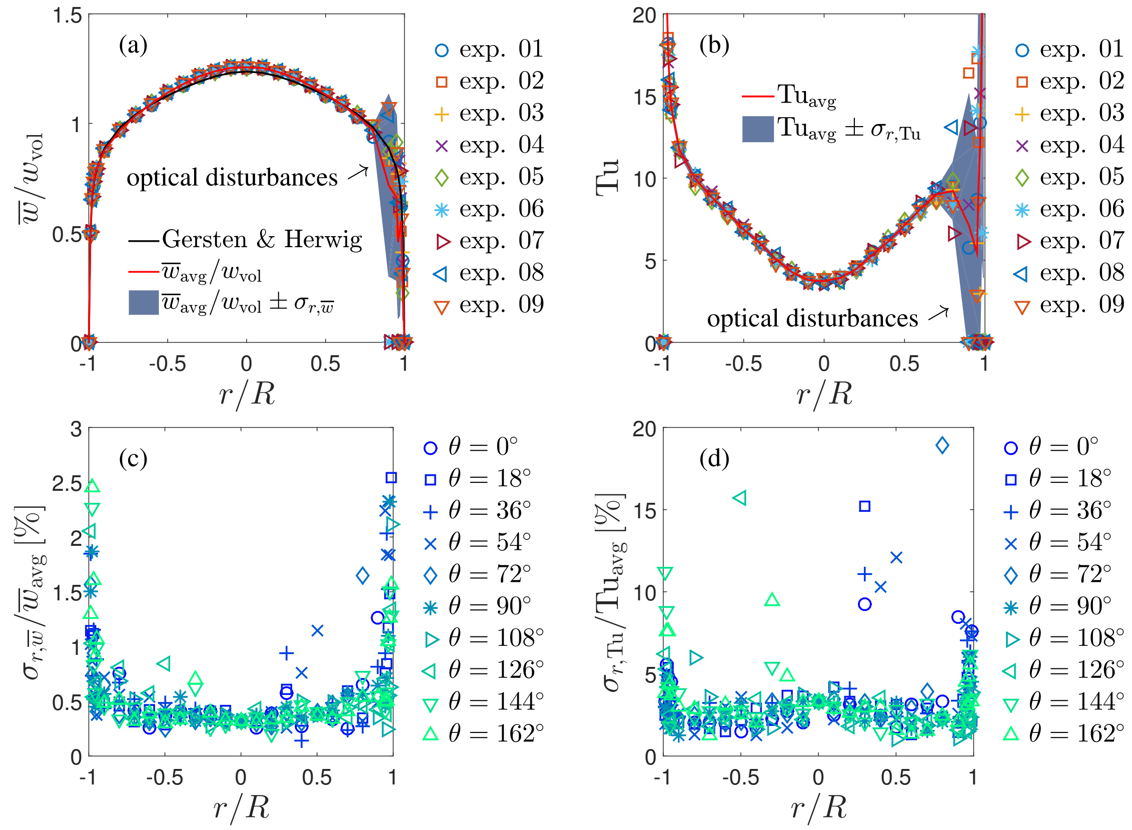

Fig. 2. Local repeatability of LDV experiments: (a) Normalized velocity $\overline{w}/w_{\mathrm{vol}}$ for a representative profile ($\theta = 72°$), (b) turbulence intensity Tu for a representative profile ($\theta = 72°$), (c) repeatability standard deviation $\sigma_{r,\overline{w}}$ (in percentage of $\overline{w}_{\mathrm{avg}}$) for all profiles, (d) repeatability standard deviation of $\sigma_{r,\mathrm{Tu}}$ (in percentage of $\mathrm{Tu}_{\mathrm{avg}}$) for all profiles. In panels (a) and (b), the markers correspond to $n = 9$ repeated measurements of the same profile, the red line is the average of repeated measurements, and the shaded area indicates the repeatability standard deviation. In panels (c) and (d), the markers correspond to repeatability standard deviations of different profiles.

In view of (6), the overall volume flow-rate (5) can be estimated through

$$Q_m = \frac{1}{N_\theta} \sum Q_i, \tag{7}$$

where the integral in (6) needs to be approximated with a suitable numerical integration scheme. Here, we use the second-order trapezoidal rule and no additional wall approximation or profile reconstruction.

All repeatabilities are quantified as standard deviations of consecutive experiments. In particular, $\sigma_{r,\overline{w}}$ and $\sigma_{r,\mathrm{Tu}}$ denote the repeatability standard deviations of single point measurements of $\overline{w}$ and Tu, respectively. Similarly, σ_{r,Q_m} denotes the repeatability standard deviation of the volume flow-rate (7). Notice that all repeatability standard deviations are defined analogously to (4) such that

$$\sigma_{r,\overline{w}} = \left(\frac{1}{n_{\mathrm{exp}} - 1} \sum_{k=1}^{n_{\mathrm{exp}}} (\overline{w}_k - \overline{w}_{\mathrm{avg}})^2 \right)^{1/2}, \tag{8}$$

where $n_{\mathrm{exp}} = 9$ is the number of consecutive experiments realized under repeatability conditions, $\overline{w}_k$ is the estimator of the single-point mean velocity (2) associated with experiment k, and

$$\overline{w}_{\mathrm{avg}} = \frac{1}{n_{\mathrm{exp}}} \sum_{k=1}^{n_{\mathrm{exp}}} \overline{w}_k \tag{9}$$

is the average of single-point mean velocities of consecutive experiments. Notice that no coverage factors are applied to the repeatability standard deviations (8).

3.1. Repeatability of local single-point measurements

In Fig. 2, we show the single-point repeatability standard deviations of experiments with pipe diameter $D = 20.0\,\mathrm{mm}$ and Reynolds number $\mathrm{Re} = 4.0 \cdot 10^4$. Panel (a) shows repeated measurements of a representative velocity profile ($\theta = 72°$). The associated repeatability standard deviation of this profile is indicated through the shaded area. Panel (c) show the repeatability standard deviations for all profiles, where the different markers correspond to different profiles in the measurement cross-section. Panels (b) and (d) displays analogous data for the turbulence intensity. Notice that increasing repeatability standard deviations in panels (c) and (d) correspond to deceasing repeatability.

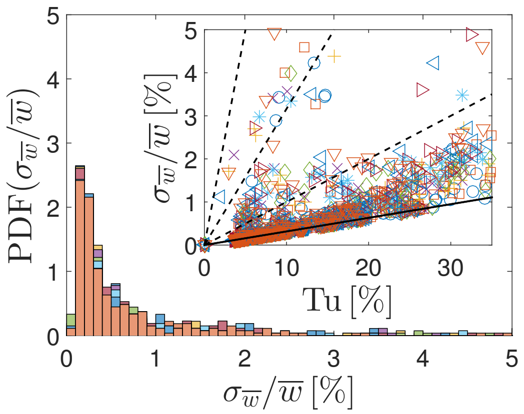

Fig. 3. Distribution of standard errors for single-point measurements: Probability density distribution (PDF) of the standard error (12) for all measurement series (same marker and color coding as in Fig. 2 (a) and (b)) along with scatter plot of standard errors (12) versus turbulence intensity (3) (inset).

The local repeatability standard deviations are approximately constant within the core region $-0.8 \leq r/R \leq 0.8$, where we find (Fig. 2 (c))

$$\sigma_{r,\overline{w}}/\overline{w}_{\text{avg}} \approx 0.5\,\%. \tag{10}$$

Similarly, the repeatability standard deviations of the turbulence intensity is approximately constant within the core region $-0.8 \leq r/R \leq 0.8$ and takes values around (Fig. 2 (d))

$$\sigma_{r,\text{Tu}}/\text{Tu}_{\text{avg}} \approx 3.0\,\%. \tag{11}$$

However, the repeatability deteriorates towards the outer regions, and measurements close to the wall are de-facto unrepeatable with repeatability standard deviations around 10–$100\,\%$ for $\sigma_{r,\overline{w}}$ and even higher values for $\sigma_{r,\text{Tu}}$ (not shown due to the axis ranges of Fig. 2 (c) and (d)).

3.2. Repeatability of the volume flow-rate

In Table 1, we show the overall volume flow flow-rate (7), where $Q_{m,\text{avg}}$ is the average of repeated experiments. We find a repeatability standard deviation of Q_m around $0.59\,\%$. In conclusion, the global repeatability of Q_m is of similar magnitude as the repeatability of individual point measurements. This indicates that individual points with poor repeatabilities appear to have only a weak impact on the repeatability of the volume flow-rate.

Table 1. Repeatability of Q_m.

Re	Q	$Q_{m,\text{avg}}$	$\sigma_{r,Q_m}/Q_{m,\text{avg}}$
$[-]$	$[\text{m}^3/\text{h}]$	$[\text{m}^3/\text{h}]$	[%]
$4.0 \cdot 10^4$	2.2728	$2.2476\,\text{m}^3/\text{h}$	0.59%

4. INTERPRETATION OF REPEATABILITY STANDARD DEVIATION

The determined repeatabilities provide experimental evidence and practical guidelines for the interpretation of LDV experiments. As discussed in ISO 21748 [2], different notions of how to account for repeatability and reproducibility in uncertainty budgets exist. For example, the GUM approach allows for a separate repeatability and reproducibility contribution to the combined uncertainty, whereas ISO 21748 [2] suggests that experimentally observed repeatability and reproducibility variance is a direct estimate of the same overall uncertainty. Alternatively, experimental uncertainty evaluation through repeatability and reproducibility studies may be used to verify the underlying mathematical models and detect incomplete or unknown effects.

In this section, we discuss how the measured uncertainty standard deviation should be interpreted and possibly integrated in revised uncertainty budgets. LDV uncertainty budgets [3–7] estimated with the GUM approach suggest that one of the largest contributions to the combined uncertainty is the standard error

$$\sigma_{\overline{w}} = \frac{\text{Tu}}{\sqrt{n}}\overline{w} \tag{12}$$

associated with the turbulence intensity and the number of single-point samples. Notice that no coverage factor is applied in the definition (12). The standard error (12) is a measure for the reliability of the estimator for the mean and depends on the flow conditions including, for example, the turbulence intensity. Since the contribution of (12) is stochastic, it is reasonable to assume that the experimentally measured repeatability standard deviation $\sigma_{r,\overline{w}}$ includes a contribution associated with (12) that is most influenced by the combination of experimental constraints (1) and flow conditions (i.e. turbulence intensity). Consequently, an assessment of uncertainty budgets according to the GUM approach may be realized through comparison of the single-point standard errors (12) to the measured repeatability standard deviations $\sigma_{r,\overline{w}}$. Such a comparison can reveal the presence of an additional repeatability contribution. Further, it will facilitate a quantification of the repeatability contribution and an assessment of whether an additional repeatability contribution should be included in a revised uncertainty budget within the GUM approach. Under the above assumptions that (12) is the largest stochastic uncertainty contribution, ideal repeatability corresponds to the scenario where the repeatability standard deviation (10) is of similar magnitude as the standard error (12). In this ideal scenario, the scatter in results of repeated experiments would be entirely due to the uncertainty associated with the standard error (12). In contrast, if $\sigma_{r,\overline{w}} > \sigma_{\overline{w}}$, an additional repeatability contribution is embodied in $\sigma_{r,\overline{w}}$ that is usually not included in uncertainty budgets following the GUM approach. Further, on recalling that the standard error is an estimate for the realiablity of the estimator of the mean and vanishes for $n \to \infty$, the true repeatability is revealed for non-zero $\sigma_{r,\overline{w}}$ in the limit $n \to \infty$.

To realize a comparison of standard error and repeatability standard deviation for the present experiments, we compute the standard error for all single-point measurements in all measurement series. In Fig. 3, we show probability density functions (PDFs) of $\sigma_{\overline{w}}$ for all single-point measurements in all measurement series and the associated scatter plot of $\sigma_{\overline{w}}$ versus Tu. The PDF in Fig. 3 shows that the majority of single-point measurements exhibit a standard error around

$$\sigma_{\overline{w}}/\overline{w} \approx 0.2\,\%. \tag{13}$$

In contrast, the repeatability standard deviation (10) discussed in Section 3.1 is larger, which points to the presence of an additional repeatability contribution. Adopting the GUM approach, the difference between (10) and (13) embodies an additional repeatability contribution that is not captured in conventional "bottom-up" uncertainty budgets of LDV systems. Hence, an additional repeatability contribution accounting for the difference between (10) and (13) could be included in a revised GUM uncertainty budget. Similarly, the present "top down" repeatability study can be used as an experimental verification of "top down" uncertainty budgets.

Notice that the present study is one specific example for one choice of parameter settings. To get a full picture, such "top-down" repeatability studies need to be repeated for every experimental setup.

5. DISCUSSION AND CONCLUSIONS

We studied the repeatability of LDV experiments for the diagnosis of flow conditions in flow benches.

Our results show that the repeatability standard deviations of single-point measurements of the mean velocity $\overline{w}$ is around $0.5\,\%$ in the core region of turbulent flow. Further, we find poor repeatability in regions close to the walls. The volume flow-rate Q_m is found to exhibit a repeatability standard deviation of $0.59\,\%$. Hence, the repeatability standard deviations of Q_m and $\overline{w}$ are of similar magnitude, suggesting that individual points with poor repeatabilities in $\overline{w}$ (for example points close to the wall) do not significantly impact the overall repeatability of the volume flow-rate.

Our results indicate that the repeatability standard deviations (10) are higher than those expected through estimating the corresponding standard errors (13). This suggests that an additional repeatability contribution could be included in uncertainty budgets of LDV experiments.

ACKNOWLEDGMENTS

Technical support from Preben Mønsted Nielsen, Thor Marun, and Salim Umar is gratefully acknowledged. DFH would like to thank Diego del Olmo Díaz, Christian Bombis, and Jens Lykke Sørensen for stimulating discussions and comments on previous versions of the manuscript.

REFERENCES

[1] *JGCM 100:2008: Evaluation of measurement data — Guide to the expression of uncertainty in measurement*. First edition, 2008.

[2] *ISO 21748: Guidance for the use of repeatability, reproducibility and trueness estimates in measurement uncertainty estimation*. 2010.

[3] D. Bublitz, S. Frank and H. E. Siekmann, "Einsatz eines Laser-Doppler-Velozimeters als Volumenstrom-Messgerät hoher Genauigkeit", *EuroHeat&Power*, vol. 25, pp. 588–598, 1996.

[4] O. Büker, *Untersuchungen zur Darstellung und Weitergabe der Skala ‚Volumen von Wasser' mithilfe laseroptischer und konventioneller Messverfahren*, PhD thesis, 2010.

[5] A. Drysdale, J. Frederiksen and M. A. Rasmussen "New on-site calibration technique for large flow meters using laser doppler velocimetry", In *Proceedings of Flowmeko 2005, Peebles, Scotland*, pp. 1–12, 2005.

[6] T. Eichler and K. Tawackolian, "Strömungsanalyse mit zwei Messtechniken und Simulationen", *EuroHeat&Power*, vol. 39, pp. 38–44, 2010.

[7] S. Frank and H. E. Siekmann, "Flow-rate measurements in asymmetric waterflows by means of laser-Doppler-velocimetry", In *Proceedings of FLOMEKO 1996, Beijing, China*, 1996.

[8] K. Gersten, "Fully developed turbulent pipe flow", In W. Menzenkirch, editor, *Fluid Mechanics of Flow Metering*, pp. 1–22, Springer, second edition, 2005.

[9] K. Gersten and H. Herwig, *Strömungsmechanik*, 1992.

[10] P. Guntermann, J. Rose, T. Lederer, M. Dues, U. Müller and A. Duckwe, "Vorort-Untersuchung von Wärmemengenzählern im Betrieb", *EuroHeat&Power*, vol. 39, pp. 44–47, 2010.

[11] U. Müller, F. Adunka, M. Dues, P. Guntermann, J. Rose and T. Lederer. "Möglichkeiten zur Vor-Ort-Überprüfung von großen Durchflusssensoren", *EuroHeat&Power*, vol. 40, pp. 52–55, 2011.

[12] U. Müller, F. Adunka, M. Dues, P. Guntermann, J. Rose and T. Lederer. "Notwendigkeiten der Vor-Ort-Überprüfung von großen Durchfluss-Sensoren" *EuroHeat&Power*, vol. 40, pp. 48–52, 2011.

[13] U. Müller, M. Dues and H. Baumann, "Vollflächige Erfassung von ungestörten und gestörten Geschwindigkeitsverteilungen in Rohrleitungen mittels der Laser-Doppler-Velocimetrie", *Technisches Messen*, vol. 74, pp. 342–352, January 2007.

[14] T. T. Yeh and G. E. Mattingly, "Pipeflow downstream of a reducer and its effects on flowmeters", *Flow Measurement and Instrumentation*, vol. 5, pp. 181–187, 1994.

[15] T. T. Yeh and G. E. Mattingly, "Laser Doppler velocimeter studies of the pipeflow produced by a generic header", *NIST Technical Note 1409*, 1995.